Coupled Calcium–Metabolism Dynamics and Lysosomal Dysfunction in Alzheimer's Disease: A Computational and Transcriptomic Analysis

Jayanth Veerappa*, Veda Kolkur†

August 2025

Abstract

Alzheimer's disease (AD) is a multifactorial neurodegenerative disorder arising from the convergence of mitochondrial dysfunction, oxidative stress, lysosomal impairment, and genetic predisposition. Here, we combine computational modeling with experimental data to uncover how disruptions in calcium and energy homeostasis contribute to disease progression. We extend the Brusselator model which is traditionally used to describe oscillatory chemical reactions to represent the Krebs Cycle, calcium influx, and insulin resistance. This nonlinear framework captures how sustained calcium overload and age-related metabolic drift lead to attenuated oscillations in the cellular energy cycle, mirroring metabolic collapse observed in AD neurons. Complementing the model, we analyzed human-derived datasets stratified by diagnosis (Control, Mild Cognitive Impairment, Early AD, Late AD). Lysosomal measurements revealed a progressive increase in lysosome number per cell from 72.3 to 104.5 and a corresponding rise in lysosomal pH from 4.49 to 5.46, consistent with impaired acidification and defective autophagy. Furthermore, a Random Forest classifier trained on gene expression profiles of key mitochondrial and lysosomal genes achieved 87% accuracy in distinguishing between diagnostic groups which reveals the predictive power of molecular signatures associated with cellular energy dysregulation and identifies potential molecular biomarkers for early AD detection.

Introduction

Alzheimer's disease (AD) is one of the most common neurodegenerative disorders, affecting about 1 in 9 people over the age of 65, with the risk increasing to nearly 1 in 3 by the time an individual reaches 85 [1]. Alzheimer's, which is commonly known for its association with memory loss, is fundamentally caused by neuronal death and progressive synaptic loss. Memories are stored in synapses, the specialized connections between neurons that allow information transfer. When synaptic loss occurs, these connections are reduced, weakening the capacity of neural circuits to encode and retrieve information, which manifests as memory impairment [5].

Neurons die primarily due to chronic neuroinflammation, which activates cellular apoptosis pathways. Tau proteins, which normally stabilize the microtubule cytoskeleton within neurons, become hyperphosphorylated and abnormal in Alzheimer's, leading to the collapse of axonal transport systems [6]. In parallel, extracellular deposits of amyloid-β peptides accumulate and form plaques, further exacerbating neuronal dysfunction. Alzheimer's also shares characteristics with prion diseases: misfolded proteins (both amyloid-β and tau) can seed misfolding of other proteins, propagating pathology throughout the brain [2].

*Emerald High School
†California High School

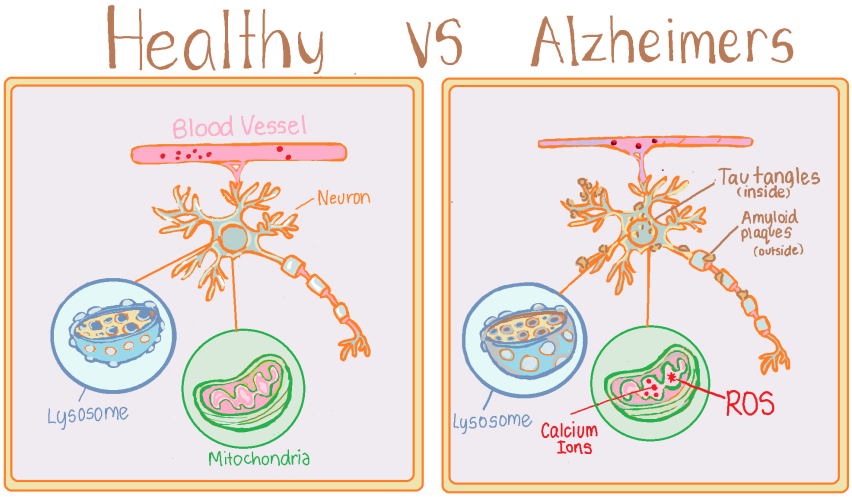

Figure 1: Healthy neurons have well-functioning mitochondria and lysosomes, while Alzheimer's neurons show amyloid plaques outside the cell, tau tangles inside, and excess calcium leading to harmful reactive oxygen species (ROS). These molecular changes disrupt energy production and damage the neuron, causing Alzheimer's disease.

Inflammation in AD is exacerbated by the dysfunction of lysosomes. Lysosomes, which act as the "garbage bags" of the cell, normally maintain an acidic environment required for enzymatic breakdown of waste. In AD, lysosomal deacidification occurs, rendering them unable to degrade toxic aggregates. This failure is closely tied to mitochondrial dysfunction. Mitochondria, the energy-producing organelles, fail to generate sufficient adenosine triphosphate (ATP), creating an energy deficit that disrupts multiple cellular processes [3].

A major contributor to mitochondrial failure is the overproduction of reactive oxygen species (ROS). These highly reactive molecules damage mitochondrial membranes, lysosomal integrity, and nuclear as well as mitochondrial DNA. ROS overproduction is driven by a hypoxic state within neurons, often caused by excessive influx of calcium ions (Ca^{2+}). While calcium is normally imported into mitochondria to increase ATP production, in AD this process becomes dysregulated, leading instead to oxidative stress and cellular toxicity.

The molecular risk is strongly influenced by genetics. The apolipoprotein E (APOE) gene plays a central role in lipid metabolism and amyloid clearance. Carriers of the $\epsilon 4$ allele have a fourfold increased risk of developing AD, whereas the $\epsilon 3$ allele is associated with baseline population risk. The rare $\epsilon 2$ allele, conversely, appears to offer some protective effects against AD [4].

So, Alzheimer's disease emerges from a cascade of pathological events: amyloid and tau misfolding, synaptic degeneration, mitochondrial dysfunction, oxidative stress, lysosomal impairment, and chronic inflammation, with genetic predisposition modulating the overall risk. These interwoven processes explain why AD is so difficult to halt once initiated and why early interventions remain an urgent priority for research.

Methods

The Brusselator Model

The Brusselator is a canonical model of nonlinear chemical oscillations originally introduced to capture autocatalytic dynamics in chemical reactions. It consists of two coupled ordinary differential equations (ODEs) describing the evolution of species $x(t)$ and $y(t)$, which interact through quadratic and cubic terms to sustain oscillations:

$$\frac{dx}{dt} = A - (B+1)x + x^2 y, \tag{1}$$
$$\frac{dy}{dt} = Bx - x^2 y. \tag{2}$$

Here, A represents a constant input feed, while B controls the effective reaction flux and thereby the oscillatory regime. In the context of cellular metabolism, the Brusselator framework provides a minimal but powerful analogy for oscillatory energy processes such as the Krebs cycle.

Krebs Cycle Analogy

To adapt the Brusselator for a metabolic interpretation, we map its variables and parameters to key intermediates and processes in the tricarboxylic acid (TCA) cycle. Table 1 summarizes the correspondence.

Brusselator	**Krebs Cycle Analogy**	**Comment**
A	Acetyl-CoA input	Constant metabolic input from glycolysis and fatty acid oxidation
B	NAD^+, ADP, etc.	Controls flux through oxidative phosphorylation; acts as regulatory factor
X	Citrate, NADH, $FADH_2$, ATP	Oscillating energy-rich intermediates produced in the cycle
Y	Oxaloacetate	Interacts with X to sustain cycle closure and regeneration
E	CO_2, heat	Dissipated by-products of metabolism
$2X + Y \to 3X$	Feedback and regeneration (oxaloacetate)	Captures the autocatalytic motif of the cycle
$X \to E$	NADH oxidation in electron transport chain	Represents energy outflow via respiration

Table 1: Mapping of Brusselator terms to Krebs cycle components.

Extended Brusselator with Calcium Influx

While the basic Brusselator captures oscillations, it omits critical regulatory layers relevant for disease modeling. To bridge this gap, we extended the model to include calcium influx, mitochondrial redox balance, insulin resistance, and age-related drift. The extended system is given by:

$$\frac{dx}{dt} = 1 - (b_{\text{eff}}(t) + 1)x + x^2 y, \tag{3}$$
$$\frac{dy}{dt} = b_{\text{eff}}(t)x - x^2 y, \tag{4}$$
$$\frac{dC}{dt} = \eta R - k_c C, \tag{5}$$
$$\frac{dR}{dt} = \gamma \frac{b_{\text{eff}} - b_0}{1 + b_{\text{eff}}/b_{\text{sat}}} - k_r R + \rho_{\text{age}}, \tag{6}$$

where the effective flux is defined as

$$b_{\text{eff}} = b_0 + hC(t).$$

In this formulation, $C(t)$ denotes cytosolic calcium influx, which directly modulates b_{eff} and thereby couples calcium signaling to oscillatory metabolism. $R(t)$ denotes insulin resistance, which

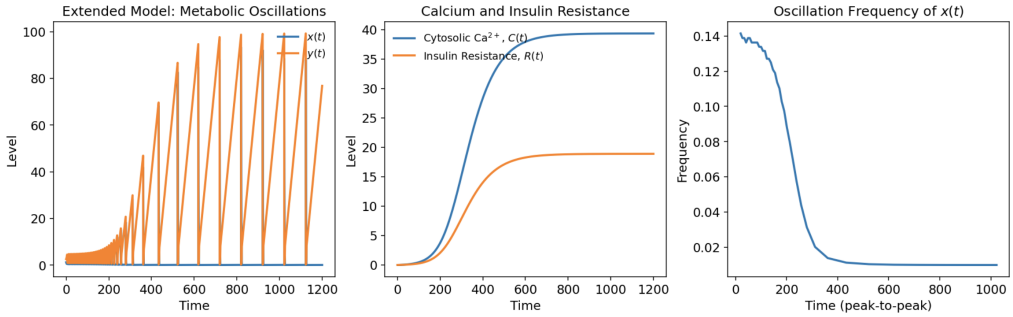

Figure 2: The extended model shows that as calcium levels and insulin resistance rise, the metabolic oscillations $x(t)$ become weaker and slower. The middle panel shows the buildup of calcium $C(t)$ and resistance $R(t)$, while the right panel highlights the gradual drop in Krebs cycle frequency, reflecting metabolic slowdown seen in Alzheimer's disease.

increases with chronic calcium stress but also saturates due to feedback. The parameters η, k_c, γ, and k_r capture calcium gain from resistance, calcium clearance, baseline resistance gain, and decay, respectively. The term ρ_{age} introduces a slow drift mimicking age-related metabolic decline.

This extended Brusselator reflects emerging evidence that mitochondrial dysfunction, calcium overload, and insulin resistance are tightly linked to cancer risk and progression. Calcium dysregulation perturbs redox balance, reduces ATP generation, and enhances oxidative stress, which in turn accelerates age-related damage. By embedding these effects into a minimal nonlinear oscillator, we provide a tractable yet biologically grounded framework to explore how cycle slowing and amplitude reduction can predispose cells toward oncogenic transformation.

Dataset Description

We also analyzed a dataset comprising human subject samples stratified by clinical diagnosis into four groups: Control, Mild Cognitive Impairment (MCI), Early Alzheimer's disease (Early AD), and Late Alzheimer's disease (Late AD). Each entry is annotated with demographic variables including age, sex, and brain region of measurement (hippocampus, temporal cortex, parietal cortex, or prefrontal cortex).

The dataset integrates molecular, cellular, and physiological variables relevant to Alzheimer's pathology. These include indices of ER–mitochondria interactions (e.g., MAM contact index, ER–mitochondria distance, and calcium flux), mitochondrial function (ROS levels, ATP concentration), lysosomal properties (pH, V-ATPase and cathepsin D activity, autophagic flux), and markers of protein aggregation and stress (Aβ42/40 ratio, Aβ oligomer concentration, phospho-tau (pTau181), ubiquitinated proteins, and lipid peroxidation products). In addition, expression levels of key genes and proteins implicated in neurodegeneration were measured, including MFN2, VAPB, PTPIP51, IP3R, VDAC1, MCU, APP, and LAMP1, along with a binary indicator for presenilin-1 mutation (PSEN1).

Results

Calcium Overload Slows and Weakens Metabolic Oscillations

Simulations of the extended Brusselator model show that rising cytosolic calcium gradually disrupts the cell's metabolic rhythm. Under baseline conditions, the metabolic variable $x(t)$ exhibits stable oscillations representing a healthy, energy-producing cycle. As calcium accumulates, these oscillations lose amplitude and become progressively slower, reflecting impaired mitochondrial redox balance and reduced ATP generation. This trend is quantified by a steady decline in the peak-to-peak oscillation frequency of $x(t)$, indicating calcium-driven metabolic slowdown (Fig. 2).

Coupling Between Calcium Accumulation and Insulin Resistance

The model also incorporates a feedback pathway in which persistent calcium elevation increases insulin resistance $R(t)$. In our simulations, calcium $C(t)$ rises rapidly, while insulin resistance grows more gradually before reaching a plateau. This joint increase destabilizes the oscillatory energy cycle and mirrors biological observations that chronic calcium dysregulation impairs metabolic flexibility in aging and Alzheimer's disease.

Lysosomal and Transcriptomic Changes Across Diagnostic Groups

Analysis of human-derived samples revealed clear signatures of lysosomal dysfunction across disease severity. Lysosome number per cell increased from 72.3 in controls to 104.5 in Late AD, and lysosomal pH rose from 4.49 to 5.46, indicating impaired acidification and reduced degradative capacity 3. These measurements align with the model's prediction that metabolic stress and calcium overload compromise downstream clearance pathways.

A Random Forest classifier trained on mitochondrial and lysosomal transcriptomic markers achieved an accuracy of 87% in distinguishing diagnostic categories (see Table 2). Genes associated with ER–mitochondria contacts, calcium handling, and autophagy contributed strongly to classification performance, suggesting that multi-system metabolic abnormalities are detectable even in early disease stages.

Using all the features in the dataset, we got an accuracy of 80% with the random forest model (see Table 3).

Class	**Precision**	**Recall**	**F1-score**	**Support**
Control	0.80	1.00	0.89	4
Early_AD	1.00	0.83	0.91	6
Late_AD	1.00	1.00	1.00	2
MCI	0.67	0.67	0.67	3
Accuracy		0.87		15

Table 2: Classification results for Random Forest model with transcriptomic features

Table 3: Classification with Random Forest model using all the features

Class	**Precision**	**Recall**	**F1-score**	**Support**
Control	1.00	1.00	1.00	4
Early_AD	0.60	0.75	0.67	4
Late_AD	0.75	1.00	0.86	3
MCI	1.00	0.50	0.67	4
Accuracy			0.80	15
Macro Avg	0.84	0.81	0.80	15
Weighted Avg	0.84	0.80	0.79	15

Conclusion

We combined a mechanistic nonlinear model with human transcriptomic and cellular data to investigate how calcium dysregulation, insulin resistance, and metabolic failure contribute to the progression of Alzheimer's disease. By extending the Brusselator framework to incorporate calcium influx, redox imbalance, and age-related metabolic drift, we demonstrated that sustained calcium overload leads to a marked slowing and weakening of metabolic oscillations. This behavior mirrors the mitochondrial dysfunction observed in Alzheimer's neurons, where elevated calcium and oxidative stress reduce ATP production and destabilize energy homeostasis.

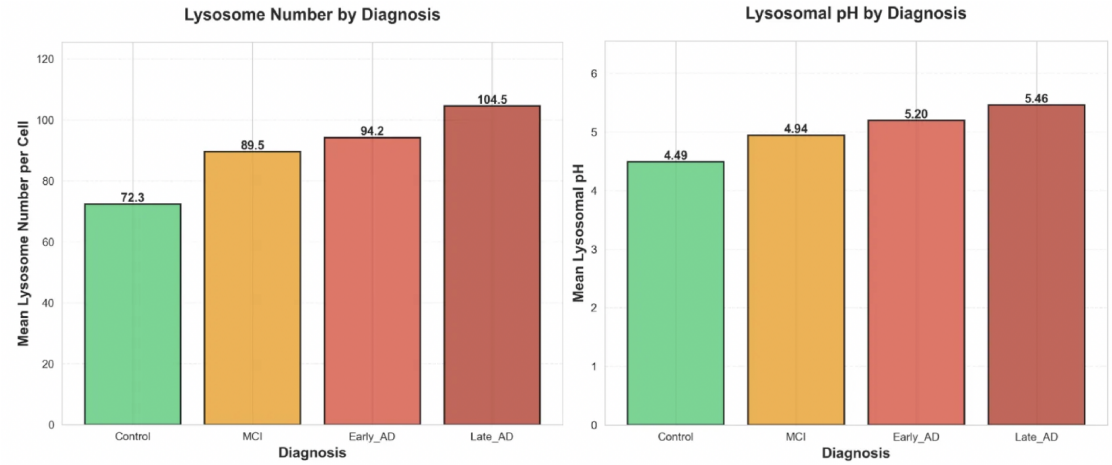

Figure 3: Lysosomal abnormalities across stages of Alzheimer's disease. (Left) Mean lysosome number per cell increases progressively from Control to MCI, Early AD, and Late AD, indicating increasing lysosomal burden with disease severity. (Right) Mean lysosomal pH also rises across diagnostic groups, reflecting impaired acidification and reduced degradative capacity.

Our analysis of human samples further supports these model predictions. Lysosomal number and lysosomal pH both increased across diagnostic stages, indicating impaired acidification and diminished degradative capacity in Alzheimer's disease. Transcriptomic classification using mitochondrial and lysosomal markers achieved 87% accuracy in distinguishing diagnostic groups, highlighting the predictive value of cellular energy and clearance pathways. When using all available molecular and physiological features, the Random Forest model achieved an accuracy of 80%, suggesting that mitochondrial, lysosomal signatures are particularly informative biomarkers.

Our modeling and experimental findings point toward a unified mechanism in which calcium overload, metabolic stress, and lysosomal failure reinforce one another to drive neurodegeneration. These results underscore the importance of early detection of metabolic dysfunction and suggest that therapeutic strategies aimed at restoring calcium balance, mitochondrial function, or lysosomal acidification may help slow or prevent Alzheimer's disease progression.

References

[1] Alzheimer's Association. "2023 Alzheimer's disease facts and figures". In: *Alzheimer's & Dementia* 19.4 (2023), pp. 1598–1695. DOI: 10.1002/alz.13013.

[2] Kim N Green and Frank M LaFerla. "Synaptic toxicity of amyloid-beta oligomers". In: *Journal of Biological Chemistry* 286.11 (2011), pp. 8617–8623. DOI: 10.1074/jbc.R110.174615.

[3] Ming Lin and M Flint Beal. "Mitochondrial dysfunction in Alzheimer's disease". In: *Nature Reviews Neuroscience* 7.5 (2006), pp. 356–372. DOI: 10.1038/nrn1909.

[4] Chia-Chen Liu et al. "APOE and Alzheimer disease: risk, mechanisms and therapy". In: *Nature Reviews Neurology* 9.2 (2013), pp. 106–118. DOI: 10.1038/nrneurol.2012.263.

[5] Dennis J Selkoe. "Alzheimer's disease is a synaptic failure". In: *Science* 298.5594 (2002), pp. 789–791. DOI: 10.1126/science.1074069.

[6] Ying Wang and Eva Mandelkow. "Tau protein in neurodegenerative disease". In: *Trends in Cell Biology* 26.6 (2016), pp. 422–433. DOI: 10.1016/j.tcb.2016.01.004.